Opto-Electronic Advances

Supplementary information

2023, Vol. 6, No. 4

DOI: 10.29026/oea.2023.220063

Flat multifunctional liquid crystal elements through multi-dimensional information multiplexing

Dongliang Tang[1†*], Zhenglong Shao[1†], Xin Xie[2†*], Yingjie Zhou[1], Xiaohu Zhang[3], Fan Fan[1*] and Shuangchun Wen[1]

[1]Key Laboratory for Micro/Nano Optoelectronic Devices of Ministry of Education & Hunan Provincial Key Laboratory of Low-Dimensional Structural Physics and Devices, School of Physics and Electronics, Hunan University, Changsha 410082, China; [2]Key Laboratory of Light Field Manipulation and Information Acquisition, Ministry of Industry and Information Technology, and Shaanxi Key Laboratory of Optical Information Technology, School of Physical Science and Technology, Northwestern Polytechnical University, Xi'an 710129, China; [3]Key Laboratory of Optoelectronic Technology and Systems of the Education Ministry of China, Chongqing University, Chongqing 400044, China.

[†]These authors contributed equally to this work.

*Correspondence: DL Tang, E-mail: dltang@hnu.edu.cn; X Xie, E-mail: xinxie@nwpu.edu.cn; F Fan, E-mail: ffan@hnu.edu.cn

This file includes:

Supplementary information for this paper is available at https://doi.org/10.29026/oea.2023.220063

Section 1: Calculations of the transfer function

The schematic of the light propagation is shown in Fig. S1, and the transfer function $H(f_x, f_y)$ can be calculated as

$$H(f_x,f_y) = \begin{cases} \exp\left[\mathrm{i}2\pi d\sqrt{1/\lambda^2 - f_x^2 - f_y^2}\right], f_x^2 + f_y^2 < 1/\lambda^2 \\ 0\ , \ \text{else} \end{cases}, \tag{S1}$$

where λ is the incident wavelength; f_x and f_y are the frequency components along x and y directions ($f_x = x/\lambda/d$, $f_y = y/\lambda/d$).

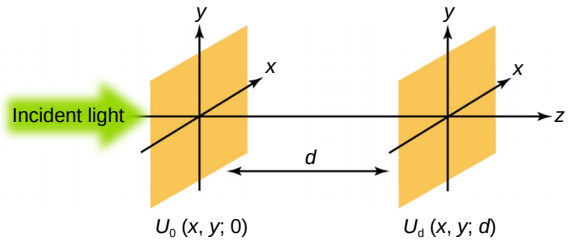

Fig. S1 | Schematic of the light propagation. Once the light field at $z = 0$ is known, the field distribution at $z = d$ can be calculated through Equation (1) in the main text.

Section 2: Duality of light modulation in an anisotropic LC molecule

When light passes through an anisotropic LC molecule, the response can be derived by using the Jones matrix formalism. If the long and short axes are along the u and v directions (Fig. 2(a) in the main text) and local u-v coordinate has a rotation angle of θ with respect to the global x-y coordinate, the Jones matrix in u-v coordinates takes the form of:

$$\mathbf{J}_{uv} = \begin{bmatrix} t_u & 0 \\ 0 & t_v \end{bmatrix}, \tag{S2}$$

where t_u and t_v are the transmission coefficients along the u and v axes. The Jones matrix in x-y coordinates can be derived through a rotation matrix $\boldsymbol{R}(\theta)$:

$$\begin{aligned} \mathbf{J}_{xy} &= \boldsymbol{R}(\theta)\mathbf{J}_{uv}\boldsymbol{R}(-\theta) = \begin{bmatrix} \cos\theta & -\sin\theta \\ \sin\theta & \cos\theta \end{bmatrix}\begin{bmatrix} t_u & 0 \\ 0 & t_v \end{bmatrix}\begin{bmatrix} \cos\theta & \sin\theta \\ -\sin\theta & \cos\theta \end{bmatrix} \\ &= \begin{bmatrix} t_u\cos^2\theta + t_v\sin^2\theta & (t_u - t_v)\sin\theta\cos\theta \\ (t_u - t_v)\sin\theta\cos\theta & t_u\sin^2\theta + t_v\cos^2\theta \end{bmatrix}. \end{aligned} \tag{S3}$$

Condition 1: if the incident light is a LP light and the polarization direction is along x-axis, the output field can be calculated as:

$$\begin{bmatrix} E_{x\text{out}} \\ E_{y\text{out}} \end{bmatrix} = \mathbf{J}_{xy}\begin{bmatrix} E_{x\text{in}} \\ E_{y\text{in}} \end{bmatrix} = \mathbf{J}_{xy}\begin{bmatrix} 1 \\ 0 \end{bmatrix} = \begin{bmatrix} t_u\cos^2\theta + t_v\sin^2\theta \\ (t_u - t_v)\sin\theta\cos\theta \end{bmatrix}. \tag{S4}$$

There exists a cross-polarized component ($E_{y\text{out}}$) in the transmitted light and the normalized intensity of $E_{y\text{out}}$ follows the relation of $\sin^2(2\theta)$. One can achieve a continuous amplitude modulation through simply controlling the LC orientation. For an arbitrary transmitted intensity, one can have four options of the LC orientation in an interval, as shown in Fig. 2(d) in the main text.

Condition 2: if the incident light is a circular polarized (CP) light, the output field can be calculated as:

$$\begin{bmatrix} E_x \\ E_y \end{bmatrix} = \frac{\mathbf{J}_{xy}}{\sqrt{2}}\begin{bmatrix} 1 \\ \pm\mathrm{i} \end{bmatrix} = \frac{1}{2\sqrt{2}}\left\{(t_u + t_v)\begin{bmatrix} 1 \\ \pm\mathrm{i} \end{bmatrix} + (t_u - t_v)\exp(\pm\mathrm{i}2\theta)\begin{bmatrix} 1 \\ \mp\mathrm{i} \end{bmatrix}\right\}. \tag{S5}$$

It is seen that LCP/RCP light would be partly converted to RCP/LCP light with an additional phase of 2θ/-2θ, which is well known as PB geometric phase.

Therefore, the anisotropic LC molecule can be used to simultaneously realize amplitude and phase modulation depending on the incident polarization state. As the normalized intensity and phase modulations are solely dependent on the molecule orientation, the elements show a wavelength-independent performance. In experiment, if t_u is considered as 1, t_v is equal to $\exp[\mathrm{i}2\pi d(n_\mathrm{e}-n_\mathrm{o})/\lambda]$, where $2\pi d(n_\mathrm{e}-n_\mathrm{o})/\lambda$ is the phase delay introduced by the birefringent LC layer, n_o, n_e, d and λ are the ordinary refractive index, extraordinary refractive index, thickness of LC layer and the working

wavelength, respectively. Once the LC material and working wavelength are determined, one can adjust the thickness of the LC layer to obtain the half-wave condition, i.e., t_v=−1 in this case.

Section 3: Genetic algorithm for the optimization of LC arrangement

The flowchart of the genetic algorithm (GA) is shown in Fig. S2. Once the near-field image is chosen, all possible arrangements of LC orientations can be calculated. And the corresponding far-field holographic image at a fixed observation plane under LCP or RCP illumination can be calculated from Eq. (1) in the main text. The cross-correlation coefficient between the possible holographic image and the target far-field image is set as the objective function in GA, and the optimization is performed using a computer with Intel i7 9700k and 32 GB memory. After about 40 hours with 600 iterations, a higher cross-correlation coefficient is achieved, and then the arrangement of LC orientations can be determined. Finally, the LC element can generate a desired near-field pattern at the sample surface under an orthogonal-polarization optical path and a far-field holographic image at the preset plane under CP illumination. The information of the observation position and working wavelength can also be added into the holographic images then optimized with the same strategy through GA.

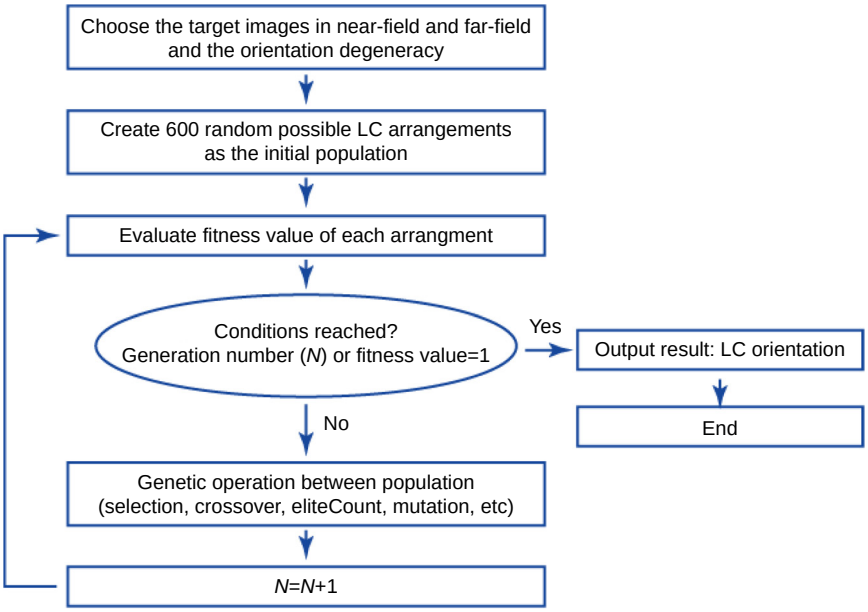

Fig. S2 | Flowchart of the GA to optimize the arrangement of LC orientations. Fitness value is defined as the cross-correlation coefficient between each possible holographic image and the target holographic image.

Section 4: A FMLCE to form two same images at near and far field

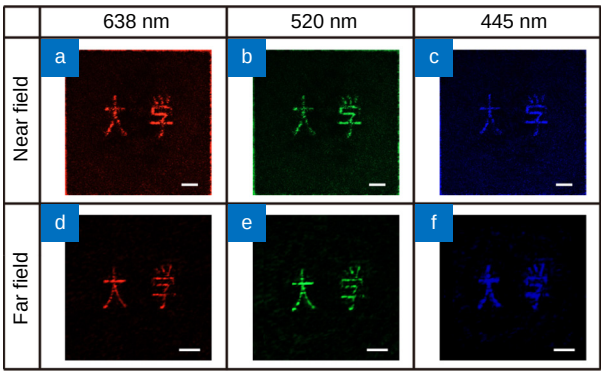

Fig. S3 | Experimental results of a FMLCE to form two same images at near and far field. (**a**–**c**) Near-field patterns are measured under an orthogonal-polarization optical path while (**d**–**f**) far-field holographic images under LCP illumination at three wavelengths of 638 nm, 520 nm and 445 nm. Scalar bars are 300 μm.

Section 5: FMLCEs to form grayscale near-field patterns and holographic images

Here, we demonstrate that the FMLCEs can be designed to form a grayscale near-field pattern and a holographic image. The optimization and fabrication processes of the element are the same with our previous FMLCEs. The experimental results are presented in Fig. S4(a). One can find that the intensity distributions are not uniform for the same grayscale value and there are some dark lines in images (the phenomenon can be also found in FMLCEs A-C). The main reason is that it is difficult for the current photoalignment technology to completely ensure that the LC molecules in each pixel (5.4 μm in this work) are in the same direction as expected, especially in adjacent areas, the alignment of LC molecules may be random or gradual due to the intermolecular force. To verify the phenomenon, a grating with only two molecular orientations (22° and −22°) is fabricated. The near-field pattern under an orthogonal-polarization optical path is shown in Fig. S4(b). Theoretically, the intensity should be equal in the whole sample. However, there are some dark regions between the area containing orientations of −22° and adjacent area containing orientations of 22°. It means that the molecular orientation in the dark regions may have a gradual change from −22° to 22°. Anyway, it is a matter of fabrication processing technology, not a matter of the design principle for our FMLCEs, and we expect the effect can be further resolved through an advanced fabrication technology.

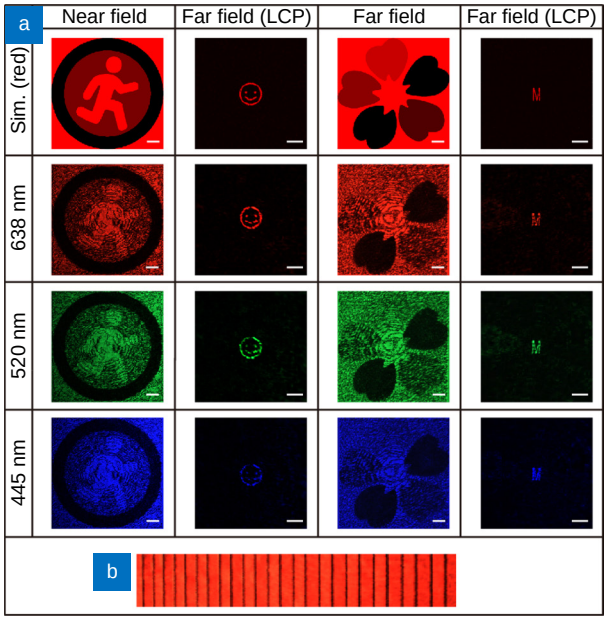

Fig. S4 | Experimental results of FMLCEs to generate grayscale near-field patterns and holographic images. (**a**) Near-field patterns are measured under an orthogonal-polarization optical path while far-field holographic images under LCP illumination at wavelengths of 638 nm, 520 nm, and 445 nm. All scalar bars are 300 μm. (**b**) Near-field pattern of a grating with two LC orientations (–22° and 22°) under an orthogonal-polarization optical path at 638 nm.

Section 6: Polarization conversion efficiency and holographic efficiency

Through changing the thickness of LC layer, the polarization conversion efficiency (PCE) can be up to 100% at a specific wavelength for CP illumination. PCE changes when the working wavelength deviates from the central wavelength. In experiment, we fabricate a polarization grating to test the PCE. The wavelength for the half-wave condition is set as 638 nm. The near-field pattern under a microscope system integrating an orthogonal-polarization optical path is shown in Fig. S5(a), and the continuous change of intensity means that LC orientations are changing continuously. PCE is measured through the setup in Fig. S5(b), where a LP light passes through the polarization grating and is deflected to −1st and +1st order, and the co-polarized light propagates to zero order. An optical power meter is used to measure light energy at ±1st order and the incident light. The PCE is calculated through the sum power of the ±1st order divided by the incident power, which equals to 47.3%, 83.7%, and 97.1% at 445 nm, 520 nm and 638 nm, respectively. The theoretical PCE is calculated as $|t_u - t_v|^2$ and the results are plotted in Fig. S5(c) (solid line). It can be seen that the experimental PCE is in good agreement with the theoretical results.

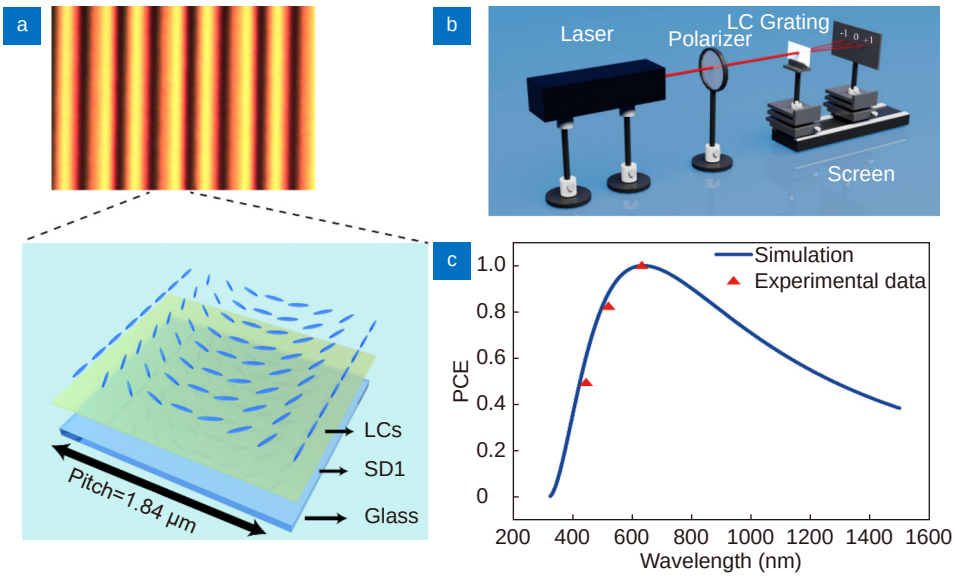

Fig. S5 | Measurement of the polarization conversion efficiency. (**a**) Image of a LC polarization grating under a microscope system integrating an orthogonal-polarization optical path. LC orientations are continuously changing in one pitch. (**b**) Home-built setup for PCE measurement. (**c**) Simulated and experimental PCE with the change of working wavelength.

The holographic efficiency is defined as the ratio between the power concentrated into the holographic image to that of the incident beam. In simulation, we superimpose the intensity inside the holographic image as the power of the holographic image, while the incident power is the sum of the intensity on the sample. In experiment, the incident light power is measured by an optical power meter before the sample. And the power of the holographic image is measured at the imaging plane. As an example, the simulated efficiency (without considering the polarization conversion) of FM-LCE A under LCP illumination is 4.7% for the three wavelengths, and the measured efficiencies are 3.4% at 638 nm, 2.7% at 520 nm, 1.6% at 445 nm, respectively. The discrepancy between the simulated (4.7%) and measured (3.4%) efficiency at 638 nm may be attributed to the fabrication and measurement errors.

Section 7: Near-field photograph under LED illumination

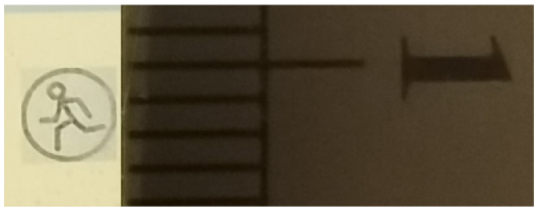

Fig. S6 | Near-field photograph of FMLCE A under the orthogonal-polarization optical path and LED illumination.

Section 8: Refractive indices of the LC material

In our fabrications, the liquid crystal material (OS1C-H1, from XAGIC Co., Ltd.) is transparent in the visible range, and the anisotropic refractive indices are shown in Fig. S7. The refractive indices at 445 nm, 520 nm and 638 nm are marked with the star symbols.

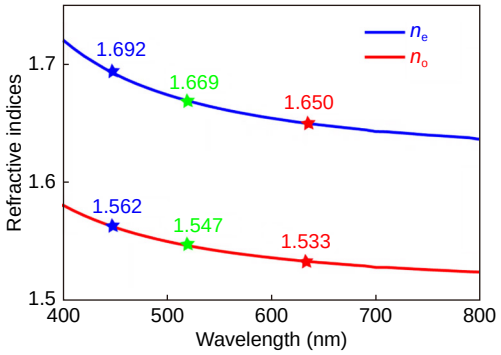

Fig. S7 | Anisotropic refractive indices of the LC material. The refractive indices at the wavelengths of 445 nm, 520 nm and 638 nm are marked with the star symbols.

Section 9: Tunable property of the multifunctional LC cell

The tunable multifunctional LC cell can be fabricated through the following processes: a) a pair of ITO glass substrates are ultrasonically cleaned, UV-Ozone bathed, and then spin-coated with a 0.5% solution of the azo-dye SD1 in dimethylformamide; b) after curing at 100 °C for 5 min, 4 μm spacers are spurted over the SD1-layer of substrates, then aligned a pair of substrates with spacer, applied AB glue to the two sides; c) put them into vacuum bags for fixing when the glue has slightly solidified to form a LC cell; d) the transfer of the target phase profile is based on our DMD photolithography system, same with the operations in Sample fabrication section; e) LCs (5CB) are injected into the LC cells, and the orientated SD1 layer will guide the LCs arrangement according to the phase profile; f) the remaining edges are sealed to complete the package.

As the external voltage gradually increases, orientations of LCs are pulled up along the direction of the electric field, and the effective birefringence gradually decreases. When the external voltage is high enough, orientations of LCs are completely pulled up, and the effective refractive index tends to n_o. In this case, the desired phase profile totally disappears and we cannot observe the near-field and far-field images.

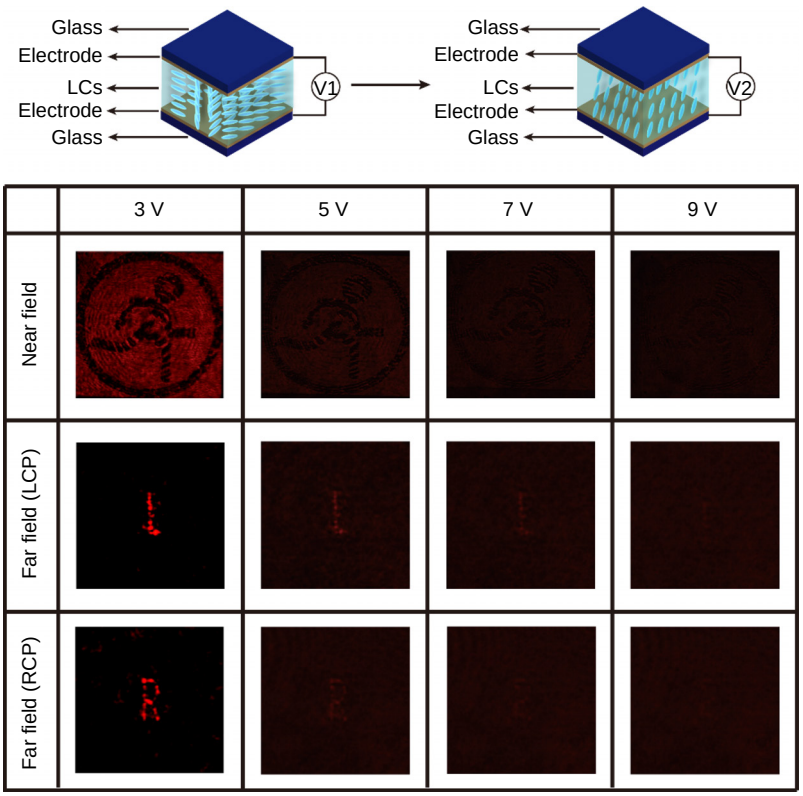

Fig. S8 | Tunable property of the polarization-multiplexing LC cell.